

CHAPTER ONE HUNDRED FIFTY TWO

SOME TECHNIQUES TO CALCULATE DESIGN CURRENTS IN SHELF AND STRATIFIED COASTAL WATERS

Stephen P. Murray* and Myron H. Young**

I. Introduction

Increasing use of marine environments for (a) petroleum-related structures (both explorational and production), (b) subsea mining (e.g., sulfur and salt), (c) brine disposal from onshore salt domes excavated for oil storage, and (d) offshore waste disposal has necessitated more frequent and more accurate predictions of current speeds and directions in coastal and shelf waters. No analytical techniques for such predictions of wind- and density-driven currents in coastal waters are presented at all in the Shore Protection Manual (1973). Wiegel (1964), however, does discuss wind-driven currents, but offers no modern methodologies for their application to coastal and ocean engineering problems.

Simple predictive models as outlined in this paper are especially valuable in feasibility studies, where the expense of a field measurement program is not yet justified. The prediction of oil spill trajectories is another important application for these procedures.

Three types of models are discussed in turn, all of which incorporate the critically important barrier effect of the coast on the current dynamics: (1) a constant eddy viscosity model, (2) an exponentially decreasing eddy viscosity model, and (3) a constant eddy viscosity model with cross-shore and longshore density gradients. The purpose of this paper is to evaluate these three models in terms of their recommended engineering usage and point out the important gaps for future research.

II. The Momentum Equations

As a first step in understanding the mechanics of the processes that drive these nearshore currents, we consider the three-component equations of motion with friction parameterized as a horizontally isotropic eddy viscosity:

*Coastal Studies Institute, Louisiana State University, Baton Rouge, LA 70803.

**Center for Wetland Resources, Louisiana State University, Baton Rouge, LA 70803.

$$\frac{du}{dt} = fv - \frac{g}{\rho} \int_{-\eta}^z \frac{\partial \rho}{\partial x} dz - g \frac{\partial \eta}{\partial x} + \frac{\partial}{\partial z} \left(K \frac{\partial^2 u}{\partial z^2} \right) \quad (1a)$$

$$\frac{dv}{dt} = -fu - \frac{g}{\rho} \int_{-\eta}^z \frac{\partial \rho}{\partial y} dz - g \frac{\partial \eta}{\partial y} + \frac{\partial}{\partial z} \left(K \frac{\partial^2 v}{\partial z^2} \right) \quad (1b)$$

$$0 = -\frac{1}{\rho} \frac{\partial p}{\partial z} + g \quad (1c)$$

In these equations u and v are speed components in the x and y directions, respectively, z is the vertical coordinate positive down, g is the acceleration of gravity, p is pressure, ρ is water density, η is the coordinate of the free surface positive upward from the mean level, and f is the Coriolis parameter. The term du/dt , dv/dt on the left side of (1a) and (1b), respectively, are the accelerations that result from the forces (per unit mass) on the right-hand side of the same equation. These forces (from left to right in the equations) represent (a) the effect of the rotation of the earth, (b) the baroclinic pressure gradient force arising from horizontal density gradients ($\partial\rho/\partial x$, $\partial\rho/\partial y$) in the water mass, (c) the barotropic pressure gradient force arising from water surface slopes ($\partial\eta/\partial x$, $\partial\eta/\partial y$), and lastly (d) the force of internal friction parameterized with an eddy viscosity (K , ν , or N).

In all three models that follow, the flow is considered quasi-steady, i.e., $\partial u/\partial t = \partial v/\partial t \approx 0$, and locally uniform, such that the convective accelerations are also negligible and thus $du/dt = dv/dt \approx 0$.

III. Constant Eddy Viscosity Model with

Negligible Horizontal Density Gradients

If the density gradients in the field are such that the baroclinic pressure gradient terms can be neglected, then (1a, b) can be written

$$K \frac{\partial^2 u}{\partial z^2} = -g \frac{\partial \eta}{\partial x} - fv, \quad (2a)$$

$$K \frac{\partial^2 v}{\partial z^2} = -g \frac{\partial \eta}{\partial y} + fu, \quad (2b)$$

where the coefficient of mixing of momentum (the eddy viscosity) K has been taken as independent of the vertical coordinate z . In shallow depths and in waters not strongly stratified in the vertical, this assumption of a three-dimensionally isotropic eddy viscosity is probably not overly restrictive. In this model x is the direction parallel to shore, positive to the right looking onshore, and u is the corresponding

speed component; y is the direction normal to the shore, positive on-shore, and v is the corresponding speed component; z is the vertical direction with an origin at mid-depth and positive downward. If the wind field is sufficiently uniform along the coast, we may expect no surface slopes in that direction, i.e., $\partial\eta/\partial x \approx 0$; then, using the complex velocity $W = u + iv$, Eq. (2) may be written

$$\kappa \frac{\partial^2 W}{\partial z^2} - fiW = i f G, \tag{3}$$

where $G = -(g/f) \partial\eta/\partial y$ is independent of z .

If the presence of the coast is taken into account by setting

$$\int_{-h/2}^{h/2} v dz = 0 ,$$

i.e., there is no net transport toward or away from the shore, the solution of (3) is

$$W = C + A \sinh jqz + jC \frac{\cosh jqz}{\sinh j\lambda}, \tag{4}$$

where $\lambda = 1/2 (qh)$, $q^2 = 1/2 (f/K)$, $j = i + 1$, A is a complex constant, and C and G are real constants.

The surface boundary condition is the usual quadratic wind stress rule:

$$\tau_s = K \rho \left[\frac{\partial W}{\partial z} \right]_s = -\kappa_s \sigma Q^2 e^{i\alpha} . \tag{5}$$

The bottom boundary condition is not the usual Ekman "no-slip" condition, which tends to considerably underestimate current speeds in shallow water, but rather a quadratic bottom friction rule:

$$\tau_b = K_b \rho \left[\frac{\partial W}{\partial z} \right]_b = -\kappa_b \rho R^2 e^{i\gamma}, \tag{6}$$

where κ_s and κ_b are friction coefficients for air-water and water-sea bottom, respectively, σ is air density, Q is the wind speed blowing at an angle α to the shoreline, and R is the current speed making an angle γ to the shoreline.

The methodology of computing the current profile in the vertical (Murray, 1975) follows:

First, the angle γ that the bottom current makes with the shoreline is determined as the root of

$$\begin{aligned} & (\cosh 4\lambda - \cos 4\lambda) \sin \gamma \left(\frac{\rho}{\sigma} \cos \alpha \cos \gamma \right)^{1/2} \frac{g^2 \kappa_s^{1/2} K}{\kappa_s} \\ & + Q \{ \cos \alpha [\sin (\gamma - \pi/4) \sinh 4\lambda - \cos (\gamma - \pi/4) \sin 4\lambda] \\ & - 2 \cos \gamma [\sin (\alpha - \pi/4) \sinh 2\lambda \cos 2\lambda \\ & - \cos (\alpha - \pi/4) \cosh 2\lambda \sin 2\lambda] \} = 0, \end{aligned} \quad (7)$$

using the Newton-Raphson technique.

Then G is determined from

$$\begin{aligned} G = R \cos \gamma + \{ & D [\cos (\gamma - \pi/4) \sinh 4\lambda \\ & + \sin (\gamma - \pi/4) \sin 4\lambda] \\ & - 2E [\cos (\alpha - \pi/4) \sinh 2\lambda \cos 2\lambda \\ & + \sin (\alpha - \pi/4) \cosh 2\lambda \sin 2\lambda] \} \\ & \times (\cosh 4\lambda - \cos 4\lambda)^{-1}, \end{aligned} \quad (8)$$

where

$$R = Q \left(\frac{\kappa_s \sigma \cos \alpha}{\kappa_b \rho \cos \gamma} \right)^{1/2}, \quad (9)$$

$$E = \frac{\cos \gamma}{\cos \alpha} D, \quad (10)$$

$$D = \frac{\kappa_b R^2}{2^{1/2} q K}. \quad (11)$$

Moreover, C , a wholly real number in (4), is given by

$$C = \frac{-[\kappa_b R^2 \sin \gamma - (\sigma/\rho) \kappa_s Q^2 \sin \alpha]}{4Kq} \quad (12)$$

and the complex coefficient A may be written

$$A = \frac{-[\kappa_b R^2 e^{i\gamma} + (\sigma/\rho) \kappa_s Q^2 e^{i\alpha}]}{2K j q \cosh j\lambda}. \quad (13)$$

Substituting (8), (12), and (13) in (4) allows the determination of vertical profiles of u and v as a function of wind speed and wind direction with respect to the coastline, eddy viscosity, total water depth, latitude, and surface and bottom friction coefficients. Note

that $\cos\alpha$ and $\cos\gamma$ must have the same sign, i.e., alongshore components of wind and bottom drift are in the same direction. When winds are from a direction between $\pi/2$ and $3\pi/2$, the sign of γ in (7) must be changed accordingly. The only poorly understood variable in this development is the eddy viscosity, which we calculated from the expression for a well-mixed surface layer (Neumann and Pierson, 1966):

$$K = 0.1825 \times 10^{-4} Q^{5/2} \rho^{-1} , \tag{14}$$

which, for wind speeds $Q < 700$ cm/sec, is in good agreement with values shown in Munk and Anderson (1948).

The results of the constant eddy viscosity theory are shown compared to three field observations from unstratified coastal water in Figures 1, 2, and 3. The agreement between theory and observation is extremely encouraging for the purpose of practical prediction. Additionally, the

$$W = 8 \text{ m/sec} , \quad \alpha = 30^\circ$$

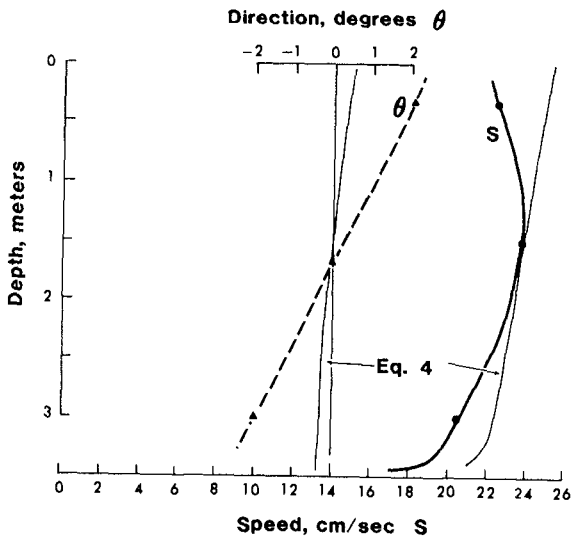


FIG. 1. Speed and direction of currents observed by Saylor (1966) under winds of 8 m/sec at 30° to the coastline compared to prediction of constant eddy viscosity theory, shown as light lines. Current direction is measured from parallel to shore-line, positive onshore.

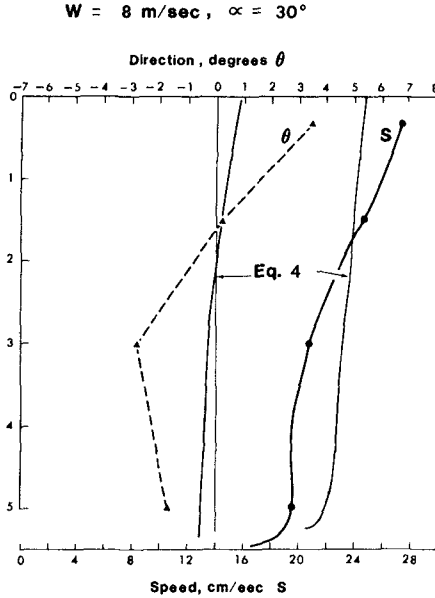


FIG. 2. As in Fig. 1.

constant eddy viscosity model has recently been used by Dr. C. J. Sonu of Tek Marine Inc. to predict the trajectory of icebergs on the Pacific continental shelf ($h \sim 30 \text{ m}$) with quite successful results (Sonu, personal communication, 1984).

An interesting point is the strong dependence of current speed on wind direction with respect to the coast. Figure 4 shows the approximately $\cos^{1/2}$ response of current speed to wind angle, a result reported earlier by Bretschneider (1967).

IV. Variable Eddy Viscosity Theory

In wind-driven current systems the energy driving the current is diffusing downward from the surface, and in moderately stratified water we expect the eddy viscosity to decrease with distance from the surface. Figure 5 shows current speed profiles off the Florida Gulf Coast in moderately stratified water. Note the steep decrease of current speed with depth, suggesting a depth-dependent eddy viscosity, an idea supported by the numerical solutions of equation (2) discussed in Murray

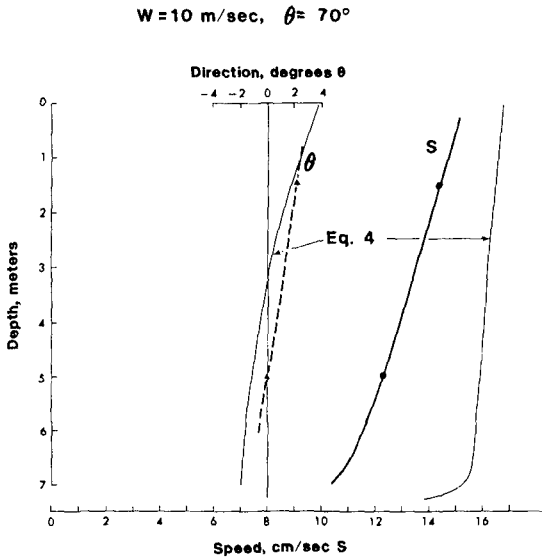


FIG. 3. As in Fig. 1, except for measurements on 11 September under winds of 10 m/sec at 73° to the coastline.

(1975). A practical predictive equation incorporating this effect was not presented, however.

Witten and Thomas (1976) addressed this problem directly with an exponentially decreasing eddy viscosity of the form $\nu = \nu_0 e^{-az}$, where ν_0 is the surface eddy viscosity and a^{-1} is the e-folding length of the eddy viscosity. Since $\lambda = ah$ is the ratio of depth to the e-folding length of the eddy, as λ gets smaller the eddy viscosity tends to be more uniform in the vertical. Large values of λ indicate a steep decrease of eddy viscosity with depth. As seen in Figure 6 at $\lambda = 0.1$, the surface value of the eddy viscosity is decreased only 5% at mid-depth, at $\lambda = 0.5$ the decrease at mid-depth is 20%, and at $\lambda = 1.0$ the decrease at mid-depth is 40%. In this model y is positive onshore, x is positive to the right looking onshore, and z and η are positive up. The complex horizontal momentum equation corresponding to (3) is

$$\frac{\partial}{\partial z} \left[A \frac{\partial W}{\partial z} \right] - i f W = g \frac{\partial \eta}{\partial n} \tag{15}$$

where $\partial/\partial n = \partial/\partial x + i \partial/\partial y$. Witten and Thomas (1976) show that (15) can

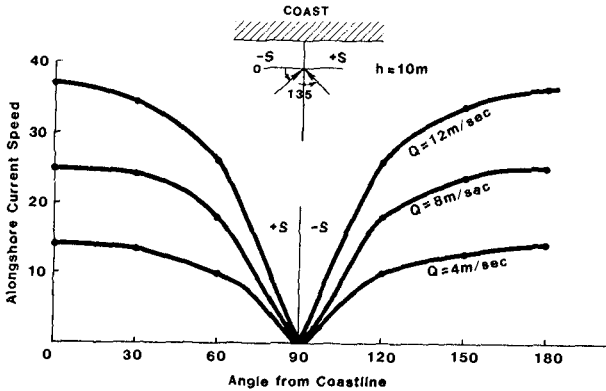


FIG. 4. The effect of changing wind angle to the coast on the alongshore current for three wind speeds (water depth = 10 m) from Eq. (4).

be put into an inhomogeneous form of the modified Bessel equation. The general solution for W then is

$$W = \zeta [AI_1(i^{1/2}\zeta) + BK_1(i^{1/2}\zeta)] + i\frac{\partial\eta}{\partial n}, \tag{16}$$

where I_1 and K_1 are the modified Bessel functions of order one, and A and B are complex constants, $\zeta = (2\alpha^{1/2}/\lambda) e^{-\lambda z/2}$, $\alpha = fh^2/\nu_0$ is the reciprocal Ekman number, and $\lambda = ah$ is the ratio of depth to e-folding length of the viscosity. The surface and bottom boundary conditions allow determination of the unknown constants A and B. Using the quadratic wind stress surface boundary condition the same as (5), but a "no slip" condition at the bottom, i.e., $W = 0$ at $z = -h$, the expressions for A and B are arrived at.

$$A = \frac{-\left\{ \frac{\lambda\tau}{2i^{1/2}} K_1 \left[\frac{2(i\alpha)^{1/2}}{\lambda} e^{\lambda h/2} \right] + \frac{\lambda i}{2\alpha^{1/2}} e^{-\lambda h/2} K_0 \left[\frac{2(i\alpha)^{1/2}}{\lambda} \right] \frac{\partial\eta}{\partial n} \right\}}{\left\{ K_0 \left[\frac{2(i\alpha)^{1/2}}{\lambda} \right] I_1 \left[\frac{2(i\alpha)^{1/2}}{\lambda} e^{\lambda h/2} \right] + I_0 \left[\frac{2(i\alpha)^{1/2}}{\lambda} \right] K_1 \left[\frac{2(i\alpha)^{1/2}}{\lambda} e^{\lambda h/2} \right] \right\}} \tag{17a}$$

$$B = \frac{\left\{ \frac{\lambda\tau}{2i^{1/2}} I_1 \left[\frac{2(i\alpha)^{1/2}}{\lambda} e^{\lambda h/2} \right] - \frac{i\lambda}{2\alpha^{1/2}} e^{-\lambda h/2} I_0 \left[\frac{2(i\alpha)^{1/2}}{\lambda} \right] \frac{\partial\eta}{\partial n} \right\}}{\left\{ K_0 \left[\frac{2(i\alpha)^{1/2}}{\lambda} \right] I_1 \left[\frac{2(i\alpha)^{1/2}}{\lambda} e^{\lambda h/2} \right] + I_0 \left[\frac{2(i\alpha)^{1/2}}{\lambda} \right] K_1 \left[\frac{2(i\alpha)^{1/2}}{\lambda} e^{\lambda h/2} \right] \right\}} \tag{17b}$$

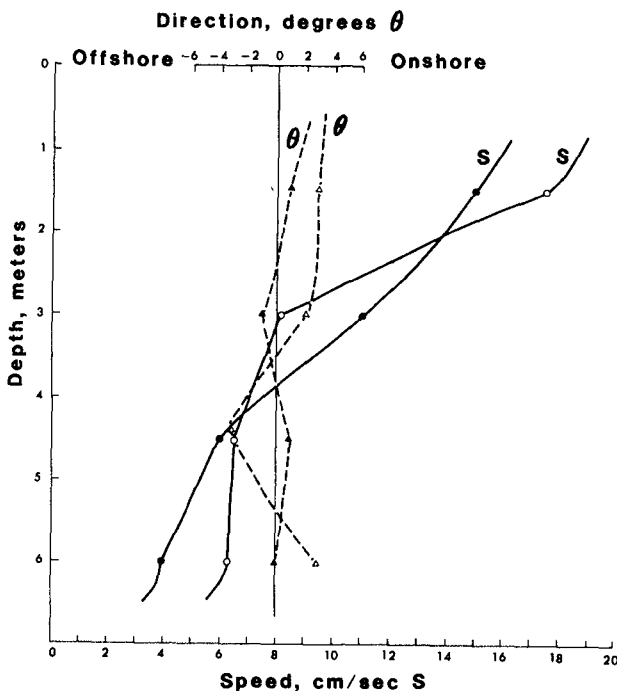


FIG. 5. Current speed (S) and direction (θ) with respect to the coast in moderately stratified water off the Florida Gulf Coast in the morning (solid dots and triangles) and the afternoon (open dots and triangles). Wind speeds are 3-4 m/sec. Note the severe kink in the afternoon speed profile due to decreased afternoon vertical mixing resulting from solar heating of the surface layer.

We solved for A and B by using the relationships between the Bessel functions and the Kelvin functions (Abramowitz and Stegun, 1972, eq. 9.9.1, 9.9.2). Using (14) for the near-surface eddy viscosity, the only unknown in (17) is the complex surface slope, $\partial\eta/\partial n$. At this point we call on our continuity condition $\int_{-n}^{\eta} v dz = 0$. Our solution procedure is to set the longshore slope $\partial\eta/\partial x = 0$, and guess a value for the cross-shore slope $\partial\eta/\partial y$, compute the constants A and B, and then compute the velocity profile from (16). Next, test to see if the continuity condition $\int_{-n}^{\eta} v dz \approx 0$ is satisfied; if it is not, iterate values of the slope

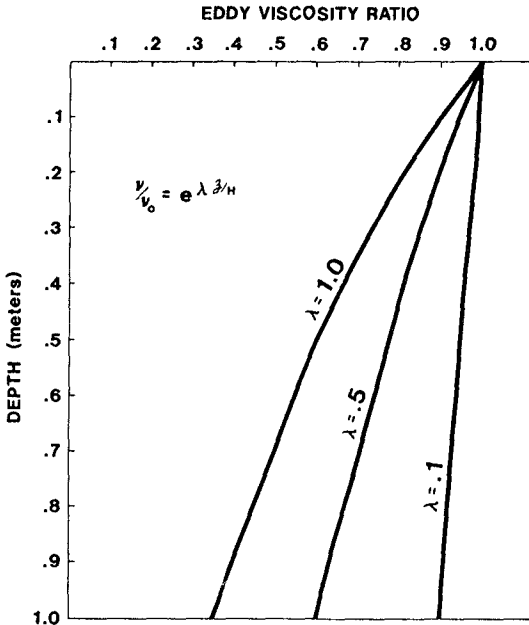


FIG. 6. The effect of λ on the vertical profile of the eddy viscosity.

until the condition is satisfied and accept the values of $\partial\eta/\partial x$, A, B, and the velocity profile as the solution.

Figure 7 gives an example of the solution from the exponential eddy viscosity theory with $\lambda = 0.1$ and 0.3 . Speeds are obviously far too low due to the no-slip bottom boundary condition. The constant eddy viscosity solution (4) is also shown for comparison. It gives a correct range of speed, but again the speed is too high near the bottom. In deeper water, Figures 8 and 9 show the two theories are tending to converge. The exponential eddy viscosity model probably gives a better representation of vertical current shear, but the actual magnitudes in the upper half of the water column are better represented by the constant ν theory. At this point we recommend the constant eddy viscosity model for shallow water (<20 m) predictions and a judicious combination of both theories for deeper water applications.

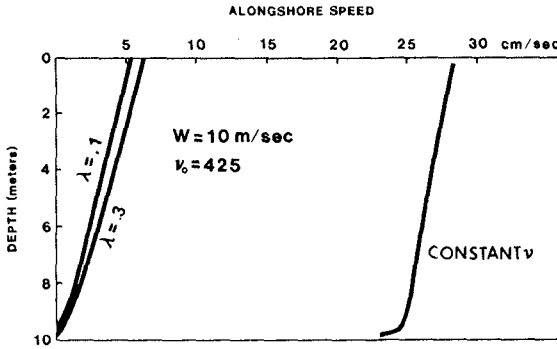


FIG. 7. Current speeds predicted by exponential decaying eddy viscosity theory compared to constant eddy viscosity theory. Wind is 10 m/sec at 45° to coast.

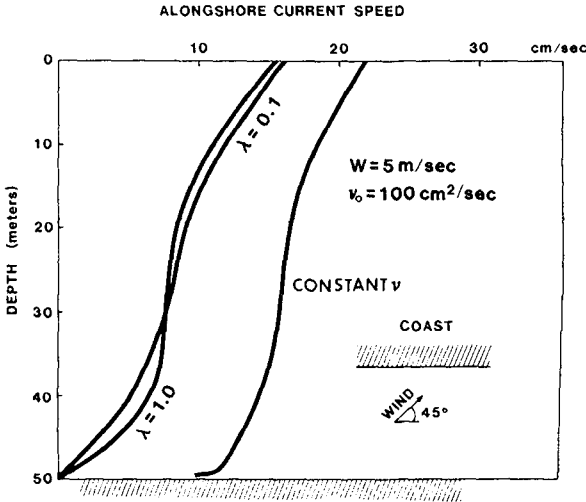


FIG. 8. As in Fig. 7, except wind is 5 m/sec at 45° to coast (deep-water example).

Clearly, the most desirable predictive scheme would incorporate features from both models. We are currently at work on the analytical solution for the wind-driven current problem incorporating both a stress bottom boundary condition and an exponentially varying eddy viscosity.

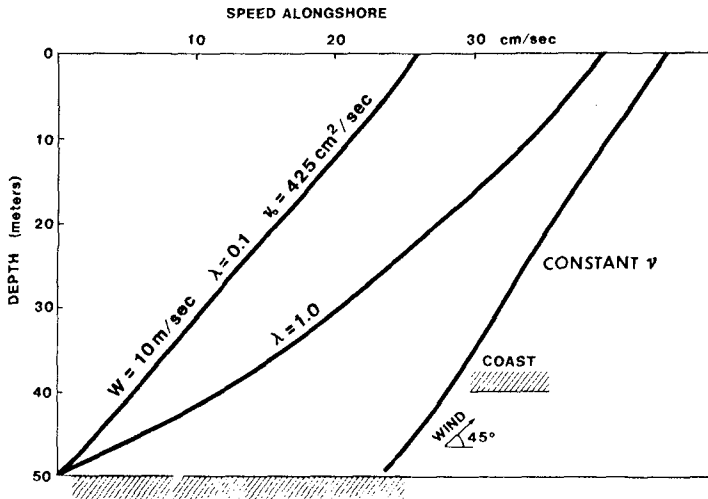


FIG. 9. As in Fig. 8, except wind is 10 m/sec at 45° to the coast (deep-water example).

V. Constant Eddy Viscosity with Horizontal Density Gradient

In many coastal regions, intense rainfall on the local watersheds produces high runoff of fresh water to the coast through a multitude of river input sources that act somewhat as a line source of fresh water along the coast. These freshwater sources typically produce a brackish, turbid band of water that frequently moves at high speeds quasi-parallel to the coast. These baroclinic coastal boundary currents are known from the southeastern coast of the United States (Blanton, 1981), the Louisiana-Texas Gulf Coast (Lewis, 1979), the Alaskan coast (Schumacher and Reed, 1980; Royer, 1979), and the Caribbean coast of Nicaragua (Murray et al., 1982). One or two truly major rivers can also produce a baroclinic coastal current stream, as in the case of the Louisiana-Texas Gulf Coast, cited above, which is the result of the massive discharges from the Mississippi and Atchafalaya Rivers.

The essential difference in the dynamics between this model and the two discussed previously is the inclusion of the baroclinic pressure gradient term. Equation (1a,b) then reduces to

$$0 = fv - \frac{z+\eta}{\rho} \frac{\partial \rho}{\partial x} - g \frac{\partial \eta}{\partial x} + N \frac{\partial^2 u}{\partial z^2} \quad (18a)$$

$$0 = -fu - g \frac{\partial \eta}{\partial y} + N \frac{\partial^2 v}{\partial z^2} \quad (18b)$$

where in this model we take z positive down, η the sea surface coordinate positive up from the mean level, h the coordinate of the bottom, N the eddy viscosity, $x(u)$ positive in the cross-shore direction toward the shore, and $y(v)$ positive in the alongshore direction, to the left of an observer looking onshore.

Again defining the complex velocity $W = u + iv$, (18a, b) can be put in the complex form

$$\frac{\partial^2 W}{\partial z^2} = \alpha^2 W - \alpha^2 \frac{ig}{f} \left\{ (z+\eta) \frac{1}{\rho} \frac{\partial \rho}{\partial x} + S \right\} \quad (19)$$

where S is the complex slope $= \partial\eta/\partial x + i (\partial\eta/\partial y)$ and $\alpha^2 = if/N$.

The solution to (19) is

$$W = A \exp \alpha(z+\eta) + B \exp -\alpha(z+\eta) + \frac{ig}{f} \left\{ \frac{z+\eta}{\rho} \frac{\partial \rho}{\partial x} + S \right\} \quad (20)$$

where A and B are complex constants to be determined by the boundary conditions. The cross-shore volume flux is given by the real part of

$$\int_{-\eta}^h W dz = \frac{A}{\alpha} (e^{\alpha h} - 1) - \frac{B}{\alpha} (e^{-\alpha h} - 1) + \frac{igh}{2\rho f} \left(\frac{\partial \rho}{\partial x} h + 2\rho S \right) \quad (21)$$

where terms in η are neglected as usual, as they affect the transport by only 0(0.1%).

The complex constants A and B and the cross-shore slope $\partial\eta/\partial x$ are considered unknown in (20). Although often considered negligible, the solution can also include a longshore baroclinic pressure gradient.

The surface boundary condition $\partial W/\partial z = -\tau_s/N$, where τ_s is complex, determines the first complex constant

$$A = B - \frac{ig}{\alpha f \rho} \frac{\partial \rho}{\partial x} - \frac{\tau_s}{\alpha N} \quad (22)$$

The bottom stress boundary condition

$$N\left(\frac{\partial W}{\partial z}\right)_h + \kappa\rho |W_h| W_h = 0 \quad (23)$$

and the continuity equation close the system by allowing computation of the constant B and the cross-shore slope $\partial\eta/\partial x$. For further details, see Murray and Young (1984).

The vertical current profile u and v can now be solved from (20) using observed or estimated values of the wind stress, eddy viscosity, water depth, cross-shelf density gradient, and longshore surface slope.

The model is evaluated by comparing our observations taken off the east coast of Nicaragua with the prediction of (20). Figure 10 shows the alongshore speed and salinity distribution in the turbid diluted coastal current found 20-30 km off the coast in this high-rainfall area (Murray et al., 1982). Our measurements of wind stress, water depth, and density structure allow us to compute a predicted velocity distribution and compare it to our field observations of current velocity. Eddy viscosities of $N = 6 \text{ cm}^2/\text{sec}$ and longshore slopes $\partial\eta/\partial y \approx 6 \times 10^{-8}$ are also estimated from the data. Pettigrew (1981) reports an eddy viscosity of $\sim 10 \text{ cm}^2/\text{sec}$ for the east coast of the U.S., so $5 \lesssim N \lesssim 15$ appears to be a good range for predictions for other coastal areas displaying similar hydrographic conditions. The longshore slope can be set = 0 unless knowledge exists to the contrary.

The distribution of the alongshore velocity component calculated from (20) and (21) under the wind stress, density gradients, and eddy viscosities associated with the field data presented in Figure 10 is given in Figure 11. Although minor details deviate, the agreement between theory and observation is extremely encouraging. For example, the magnitude and location of the current maxima at ~ 12 km offshore and the offshore length scale of 15-20 km are all successfully reproduced. The offshore countercurrent of 5-10 cm/sec in both observations and theory is apparently the result of the slight longshore surface slope opposing the wind.

The theory assumes a density gradient that is constant with depth, and thus predicts significant southerly velocity components throughout the water column. In the observations, however, the density gradient weakens with depth, leading to some overprediction of the near-bottom velocities, but the first-order approximation of the longshore speed

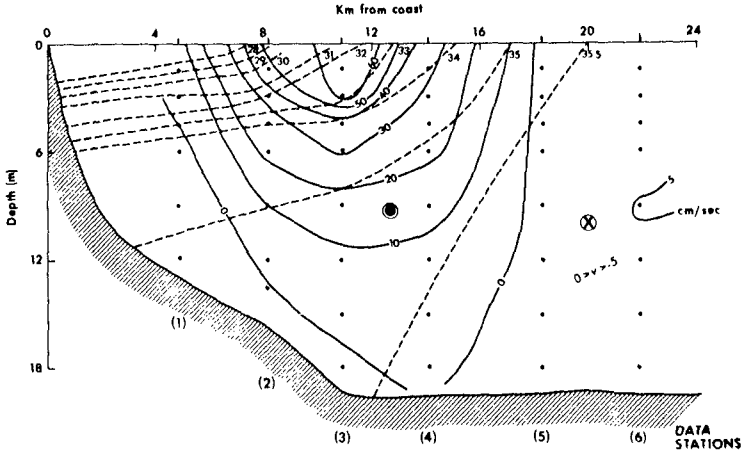


FIG. 10. Alongshore current speeds (cm/sec) observed along east coast of Nicaragua (solid lines) and coincident salinity distribution (dashed lines), which delineate the baroclinic coastal current. Dots indicate data observation points. Basic southerly flow (off page) is bordered by a weak offshore countercurrent.

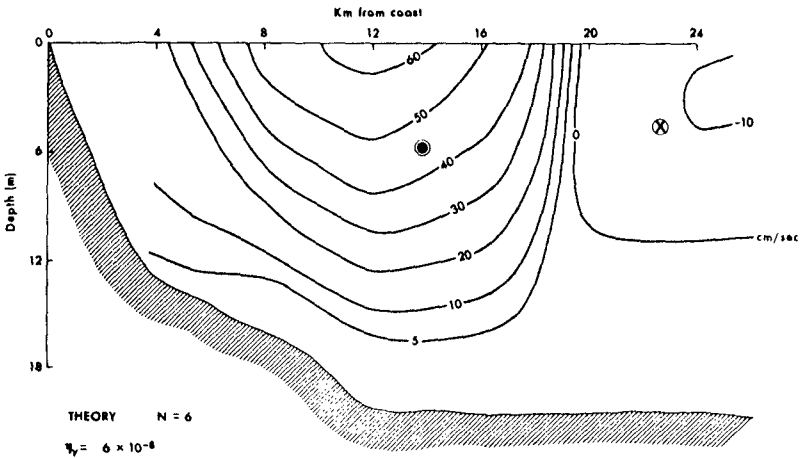


FIG. 11. Prediction of the distribution of alongshore current speeds from the theoretical model (20) under the field conditions shown in Fig. 10.

distribution, the goal of this paper, is clearly a good one.

VI. Summary

Three analytical models are presented that can be used to predict vertical profiles of coastal and inner-shelf currents when applied with careful consideration of the pertinent physical parameters in operation. Two of the models are driven solely by wind stress, while the third also incorporates density gradient effects.

An important result suggested by the successful comparison of our field data to theory is the possibility that considerable knowledge of the nearshore velocity distribution along coasts with simple geometry can be obtained, given data on local winds, from routine bathymetric and hydrographic (STD) surveys. An immediate application is the prediction of current structure for offshore petroleum operations and the trajectories of oil spill movements along many subtropical coasts as well as other high-runoff coasts such as the Pacific coast of Alaska.

Acknowledgments

This research was supported under a contract between the Coastal Sciences Program of the Office of Naval Research, Arlington, Virginia, and Louisiana State University.

References

- Abramowitz, M., and Stegun, I. A., Handbook of Mathematical Functions, National Bureau of Standards Applied Mathematics Series, No. 55, 1972, 1945 pp. (also available from Dover Publishing Company).
- Blanton, J. O., "Ocean Currents along a Nearshore Frontal Zone on the Continental Shelf of the Southeastern United States," Journal of Physical Oceanography, Vol. 11, No. 12, 1981, pp. 1627-1637.
- Bretschneider, C. L., "On the Generation of Wind-Driven Currents over the Continental Shelf," The New Thrust Seaward, Transactions, of the Third Marine Technology Society Conference, San Diego, pp. 96-113.
- Lewis, J. K., "Coastal Frontal Systems as a Pollutant Control Mechanism for Offshore Energy Production," Proceedings of the Marine Technology Society Meeting, New Orleans, 1979, pp. 389-396.
- Munk, W. H., and Anderson, E. R., "Notes on a Theory of the Thermocline," Journal of Marine Research, Vol. 7, 1948, pp. 276-295.
- Murray, S. P., "Trajectories and Speeds of Wind-Driven Current near the Coast," Journal of Physical Oceanography, Vol. 4, 1975, pp. 347-360.

- Murray, S. P., and Young, M. H., "The Nearshore Current along a High-Rainfall, Trade Wind Coast - Nicaragua," Coastal, Estuarine, and Shelf Science (in press).
- Murray, S. P., Hsu, S. A., Roberts, H. H., Owens, E. H., and Crout, R. L., "Physical Processes and Sedimentation on a Broad, Shallow Bank," Estuarine, Coastal, and Shelf Science, Vol. 14, 1982, pp. 135-157.
- Neumann, G., and Pierson, W. J., Jr., Principles of Physical Oceanography, Prentice-Hall, 1966, 454 pp.
- Royer, T. C., "On the Effect of Precipitation and Runoff on Coastal Circulation in the Gulf of Alaska," Journal of Physical Oceanography, Vol. 9, No. 3, 1979, pp. 555-563.
- Saylor, J. H., "Currents at Little Lake Harbor, U.S. Lake Survey Research Report No. 1-1, Lake Survey District, Corps of Engineers, Detroit, Michigan, 1966, 19 pp.
- Schumacher, J. D., and Reed, R. K., "Coastal Flow in the Northwest Gulf of Alaska: The Kenai Current," Journal of Geophysical Research, Vol. 85, No. C11, 1980, pp. 6680-6688.
- Shore Protection Manual, U.S. Army Coastal Engineering Research Center, U.S. Government Printing Office, Washington, D.C., 1973.
- Wiegel, R. L., Oceanographical Engineering, Prentice Hall, New York, 1964, 532 pp.
- Witten, A. J., and Thomas, J. H., "Steady Wind Driven Currents in a Large Lake with a Depth Dependent Eddy Viscosity," Journal of Physical Oceanography, Vol. 6, No. 1, 1976, pp. 85-92.